Annals of Nuclear Medicine
https://doi.org/10.1007/s12149-019-01386-1

ORIGINAL ARTICLE

Fully automated analysis for bone scintigraphy with artificial neural network: usefulness of bone scan index (BSI) in breast cancer

Anri Inaki[1] · Kenichi Nakajima[2] · Hiroshi Wakabayashi[1] · Takafumi Mochizuki[3] · Seigo Kinuya[4]

Received: 7 April 2019 / Accepted: 11 July 2019

Abstract

Objective Artificial neural network (ANN) technology has been developed for clinical use to analyze bone scintigraphy with metastatic bone tumors. It has been reported to improve diagnostic accuracy and reproducibility especially in cases of prostate cancer. The aim of this study was to evaluate the diagnostic usefulness of quantitative bone scintigraphy with ANN in patients having breast cancer.

Patients and methods We retrospectively evaluated 88 patients having breast cancer who underwent both bone scintigraphy and ^{18}F-fluorodeoxyglucose (FDG) positron-emission computed tomography/X-ray computed tomography (PET/CT) within an interval of 8 weeks between both examinations for comparison. The whole-body bone images were analyzed with fully automated software that was customized according to a Japanese multicenter database. The region of interest for FDG-PET was set to bone lesions in patients with bone metastasis, while the bone marrow of the ilium and the vertebra was used in patients without bone metastasis.

Results Thirty of 88 patients had bone metastasis. Extent of disease, bone scan index (BSI) which indicate severity of bone metastasis, the maximum standardized uptake value (SUVmax), metabolic tumor volume (MTV), total lesion glycolysis (TLG), and serum tumor markers in patients with bone metastasis were significantly higher than those in patients without metastasis. The Kaplan–Meier survival curve showed that the overall survival of the lower BSI group was longer than that with the higher BSI group in patients with visceral metastasis. In the multivariate Cox proportional hazard model, BSI (hazard ratio (HR): 19.15, $p=0.0077$) and SUVmax (HR: 10.12, $p=0.0068$) were prognostic factors in patients without visceral metastasis, while the BSI was only a prognostic factor in patients with visceral metastasis (HR: 7.88, $p=0.0084$), when dividing the sample into two groups with each mean value in patients with bone metastasis.

Conclusion BSI, an easily and automatically calculated parameter, was a well prognostic factor in patients with visceral metastasis as well as without visceral metastasis from breast cancer.

Keywords Artificial neural network · Breast cancer with bone metastasis · Bone scan · FDG-PET

Introduction

Patients having metastatic breast cancer (classified as stage IV in the American Joint Committee on Cancer staging) has an extremely poor prognosis, although some factors such as race, heredity, and the presence of hormone receptors have been reported to influence a patient's prognosis. Approximately 70% of patients who died from breast cancer had bone metastases at autopsy [1], while the 5-year survival of patients with metastatic breast cancer is less than 20%. Moreover, bone metastasis may cause swelling, severe pain, and pathological fractures, which influence a patient's quality of life.

Bone scintigraphy has been used for several decades as a diagnostic tool for several types of bone lesions, especially metastatic bone tumors. Recently, single-photon computed tomography combined with X-ray computed tomography (SPECT/CT) has become more established and improved diagnostic accuracy although whole-body imaging is still used for detecting the presence of bone metastasis both easily and practically [2, 3]. However, the accuracy of the bone scan depends on the ability of nuclear medicine physicians or radiologists because its interpretation is performed on visual judgment based on their clinical experience. While

✉ Anri Inaki
henri@staff.kanazawa-u.ac.jp

Extended author information available on the last page of the article

Published online: 17 July 2019

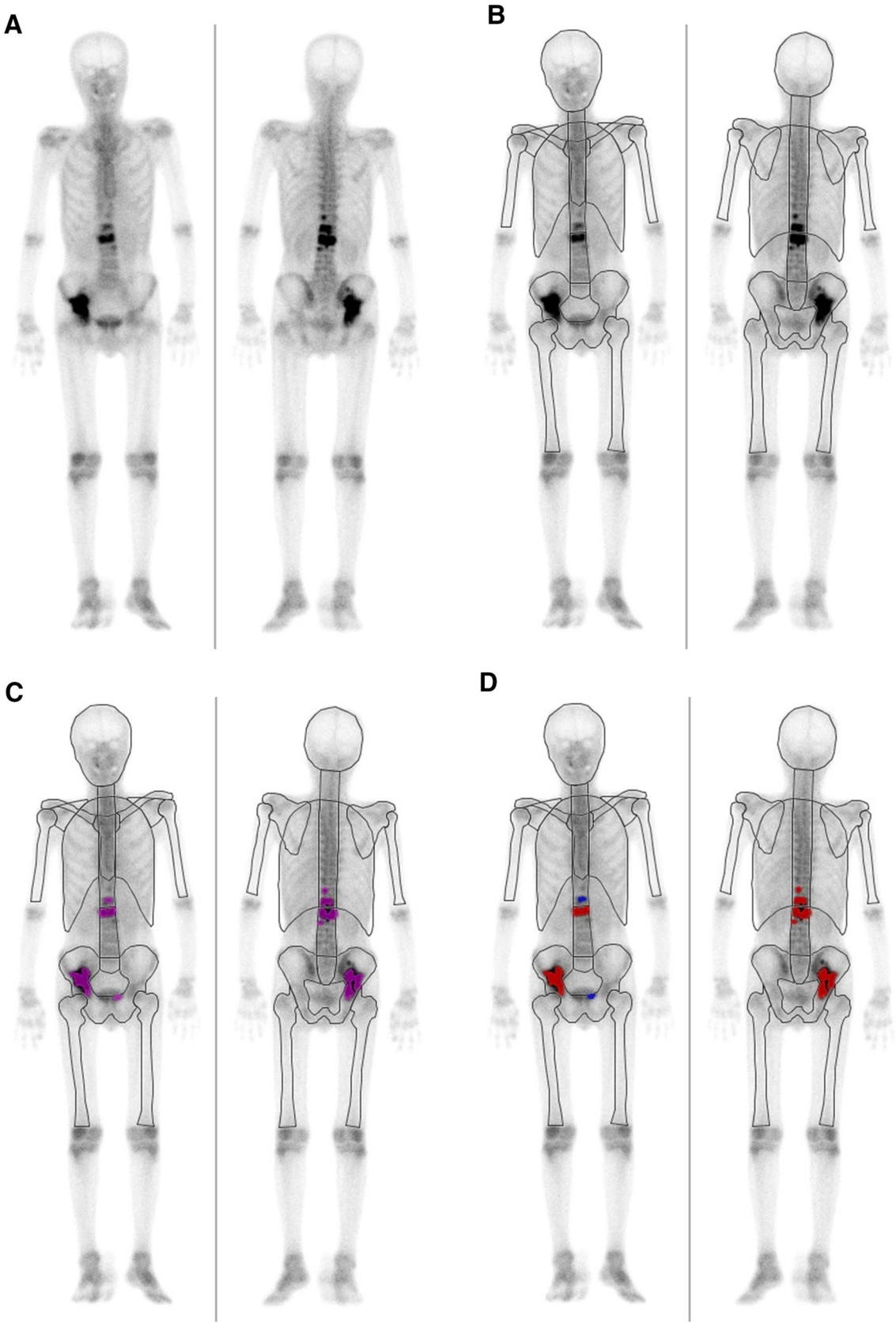
A
B
C
D

◂**Fig. 1** Visualized analysis procedure. An original image **a** is segmented into 22 areas (**b**). After detection of suspicious regions (purple on **c**), all hot spots are scored from 0 to 1 in accordance with ANN and those with an ANN value of 0.5 or higher are judged as being possible metastatic lesions (red on **d**). The occupied rates of all possible metastatic lesions (regional BSI: rBSI) are summed up as BSI (**e**). The process is fully automated and is therefore always reproducible

some objective methods have been proposed to evaluate bone scanning, the bone scan index (BSI) based on artificial neural network (ANN) technology has been established clinically for a quantitative and reproducible indicator.

The BSI was proposed at the Memorial Sloan Kettering Cancer Center and was developed as a marker to assess the extent of bone metastasis [4, 5]. Over the last several years, the BSI based on ANN technology has shown great promise in analyzing bone scintigraphy for metastatic bone tumors and has been reported to improve its diagnostic accuracy and reproducibility especially in prostate cancer [6, 7]. The original software for the ANN analysis was released as EXINI bone (EXINI Diagnostics AB, Lund, Sweden) and then as revised software called BONENAVI (FUJIFILM Toyama Chemical, Co. Ltd, Tokyo, Japan), which was retrained from EXINI bone by using a large number of Japanese multicenter databases. The revised version clearly improved the diagnostic accuracy in patients with metastatic bone tumors [8]. However, there have only been a few studies on the relationship between skeletal-related events (SRE) and the BSI in breast cancer [9], while fewer studies still have reported on the prognostic value of the BSI in accordance with diagnostic accuracy and survival rate.

The aim of this study was to clarify the diagnostic accuracy of ANN analysis and also to evaluate its prognostic value in patients with metastatic breast cancer. The diagnostic ability was compared with a five-point scale for extent of disease (EOD) reported by Soloway et al. [10] and ^{18}F-fluorodeoxyglucose (FDG) positron-emission tomography (PET), which have been widely utilized in clinical practice.

Materials and methods

Patients

We retrospectively evaluated patients with breast carcinoma who underwent bone scintigraphy or ^{18}F-FDG-PET/CT in our institute from 2007 to 2012 and found 2187 examinations (763 subjects) and 1572 examinations (659 subjects), respectively. In these patients, we adopted the patients who had underwent surgical resection of the primary tumor and had not been received chemotherapy at the time of examinations. Moreover, for the comparison of bone scintigraphy and FDG-PET study, we extracted subjects who underwent both tests within 8 weeks of each other in order to compare the examinations under the same disease conditions. The subjects who had any systemic bone diseases were excluded. The bloods of all the patients were also analyzed including serum creatinine, serum calcium, alkaline phosphatase (ALP), carcinoembryonic antigen (CEA), and carbohydrate antigen 15-3 (CA15-3). The presence of bone metastasis was proven by any diagnostic images including CT, bone scan, FDG-PET, and magnetic resonance imaging (MRI).

The present study was approved by the ethics committee of Kanazawa University. Since this was a retrospective study, written informed consent from each patient was waived, while the patients were provided an opportunity to opt out of this study by disclosing the details of this study on website in accordance with the Ethical Guidelines for Medical and Health Research Involving Human Subjects [11].

Bone scan imaging

Whole-body anterior and posterior imaging was performed for approximately 15 min (scan speed: 15 cm/min) after 3–4 h of intravenous injection of 740 MBq ^{99m}Tc-methylene diphosphonate (MDP; FUJIFILM Toyama Chemical Co., Ltd., Tokyo, Japan). All images were obtained by an e.cam dual-headed gamma camera (Siemens Healthcare GmbH, Munich, Germany) equipped with a low-energy, high-resolution, parallel-hole collimator. The energy peak was centered at 140 keV with 15% windows, and the matrix size was 256×1024.

Bone scan analysis

The analysis of the whole-body image was automatically carried out with BONENAVI (FUJIFILM Toyama Chemical, Co. Ltd, Tokyo, Japan), which was customized from EXINI bone (EXINI Diagnostics AB, Lund, Sweden) according to a Japanese multicenter database [6]. The automated algorithm for the analysis has been described previously [12]. In brief, the analysis in this software was performed with ANN technology, which was constructed by supervised learning (Fig. 1). First, the skeleton atlas in the software was aligned to a patient's anterior and posterior images in accordance with Morphon registration [13], a kind of non-rigid deformation method. Second, all hot spots were detected in 12 anterior and 10 posterior anatomically segmented regions in the skeleton atlas. Third, each hot spot was quantified and denoted by a value from 0 (non-metastatic) to 1 (metastatic), which is called the ANN value, corresponding to the probability of abnormality. Finally, all hot spots with an ANN value of 0.5 or higher (possible metastasis) were determined, and the BSI was calculated as the percentage of the metastatic region to the whole skeleton. The number of

the positive hot spots was also expressed by Hsn. For comparison, the images were evaluated with two expert nuclear physicians according to EOD grade classification and the average scores were adopted.

^{18}F-FDG-PET imaging and analysis

All patients fasted for approximately 6 h before ^{18}F-FDG administration and PET/CT imaging. The blood glucose level was examined before ^{18}F-FDG injection and had to be less than 120 mg/dL. Whole-body PET/CT scanning was examined with Discovery ST Elite or Discovery PET/CT 690 (GE Healthcare, Little Chalfont, UK). An emission scan was performed in three-dimensional mode at a rate of 2 min/bed station after 60 min of intravenous injection of 4.0 MBq/kg ^{18}F-FDG. PET had a 500-mm transaxial field of view (FOV) and a 158-mm axial FOV. Unenhanced CT scanning was also performed for attenuation correction and image diagnosis. Emission images were reconstructed using a three-dimensional ordered-subset expectation maximization algorithm with matrix size 128×128, two iterations and 20 subsets (Discovery ST Elite) or two iterations and 18 subsets (Discovery PET/CT 690). After reconstruction, a 5-mm full-width at half-maximum Gaussian post-filter and CT attenuation correction was applied. The region of interest (ROI) of FDG-PET was set for bone lesions that have the highest value of the maximum standardized uptake value (SUVmax) in the patients with bone metastasis and bone marrow of the ilium and the vertebra in patients without bone metastasis. Additionally, metabolic tumor volume (MTV) and total lesion glycolysis (TLG) was calculated. In accordance with EANM procedure guidelines for tumor imaging [14], voxels with 41% or more of the SUVmax of the VOI in the each lesion were incorporated to define the volume of each lesion.

Statistical analysis

All the patients were divided into two groups based on the presence of bone metastasis. To compare characteristics of each group, the Student's *t* test and Pearson's *Chi-square* test and Fisher's exact test for test of independence were used. The difference in the mean values between groups was determined by the Student's *t* test. The significance of the difference between two proportions were assessed by Pearson's *Chi-square* test in common and Fisher's exact test for small sample size less than 10 in contingency tables. The area under the curve (AUC) including the receiver operating characteristics (ROC) curve was estimated to evaluate the diagnostic accuracy of bone metastasis. Optimal cutoff point was calculated by Youden's index (maximum of sensitivity—(1–specificity)). Comparing each AUC was performed with the method of DeLong et al. [15]. The patients were divided into two groups using the mean values of patients with bone metastasis. Kaplan–Meier survival curves were used in order to visualize the time to event (either death or censoring) while overall survival was compared using the log-rank test. Each covariate was analyzed by the Cox proportional hazards model to evaluate their contribution to events. Hazard ratios were calculated with their 95% confidence interval (CI). Significant factors by univariate Cox hazards model ($p < 0.05$) were analyzed for independent prognostic importance by multivariate Cox hazards model using a stepwise procedure.

We used a statistical software JMP® (SAS Institute Inc., Cary, NC, USA) for analyzing all the acquired data.

Results

The patients' demographics are shown in Table 1 and 2. There were 88 eligible subjects who satisfied the following conditions. In comparing patients with and without bone metastasis, no significant differences were found in age, estimated glomerular filtration rate (eGFR), interval between examinations, or ALP. Significant differences were observed between the groups regarding follow-up period, overall outcome, CEA, CA15-3, the presence of visceral metastasis, EOD, ANN value, BSI, the number of the positive hot spots, maximal value of SUVmax in bone lesions, metabolic tumor volume (MTV) and total lesion glycolysis (TLG) in the whole metastatic lesions. Serum calcium concentration in patients with bone metastasis was significantly lower than that without bone metastasis. In comparing patients with and without visceral metastasis, there were significant differences in EOD, ANN value, BSI, the number of the positive hot spots, maximal value of SUVmax at bone lesion, MTV and TLG in bone lesions.

The diagnostic accuracy of EOD, BSI, and SUVmax for identifying bone metastasis were evaluated by using ROC analysis (Fig. 2). The ROC curve AUCs were 0.898, 0.836, and 0.972 for EOD, BSI and SUVmax, respectively. The SUVmax showed a higher accuracy compared to the BSI ($p = 0.0091$) or EOD ($p = 0.0137$).

To evaluate overall survival by using the Kaplan–Meier survival curves, thresholds of EOD, BSI and TLG were set using mean values in patients with visceral metastasis (Fig. 3). In the patients without visceral metastasis, the groups with low EOD, low BSI, and low TLG showed significantly longer survival than those with high EOD, high BSI, and high TLG. In the presence of visceral metastasis, the patients with high BSI have a poorer prognosis than those with low BSI.

Based on univariate Cox proportional hazard analysis (Table 3), the patients with higher EOD (hazard ratio (HR) = 2.03), SUVmax (HR = 1.20), ANN value (HR = 5.00)

Table 1 Patients' characteristics

	With bone metastasis ($n=30$)	Without bone metastasis ($n=58$)	p value
Age (year)	56.1 ± 10.8	57.8 ± 11.0	0.4915[a]
Tumor histology			
Invasive ductal carcinoma	27	52	
Invasive lobular carcinoma	3	2	
Apocrine carcinoma	0	1	
Mucinous carcinoma	0	2	
Spindle cell carcinoma	0	1	
Interval between examinations (day)	23.3 ± 15.4	23.9 ± 15.6	0.8722[a]
Follow-up period (day)	1057.9 ± 754.2	1515.5 ± 723.8	0.0042[a]
Overall outcome			
No evidence of disease	0	38	< 0.0001[b]
Alive with disease	10	11	
Dead of disease	20	9	
Blood examination			
eGFR (mL/min/1.73 m^2)	83.8 ± 25.3	86.1 ± 16.7	0.6144[a]
ALP (IU/L)	292.7 ± 239.4	248.8 ± 94.6	0.3400[a]
Calcium (mg/dL)	9.4 ± 0.5	9.7 ± 0.4	0.0078[a]
CEA (ng/mL)	14.7 ± 23.6	3.4 ± 7.8	0.0015[a]
CA15-3 (U/mL)	62.2 ± 108.1	18.1 ± 9.1	0.0069[a]
CT findings			
Osteoblastic	8		
Osteolytic	5		
Mixed	13		
Invisible	4		
Visceral metastasis	17 (57%)	12 (21%)	0.0007[c]
Region of visceral metastasis (duplicated)			
Lung	6	5	
Liver	6	5	
Pleura	3	1	
Adrenal gland	1	0	
Soft tissue	1	2	
Peritoneum	1	1	
Skin	1	1	
Bone scintigraphy			
EOD	0.28 ± 0.35	1.78 ± 1.15	< 0.0001[a]
ANN value	0.70 ± 0.37	0.22 ± 0.32	< 0.0001[a]
BSI	1.92 ± 2.32	0.17 ± 0.36	0.0001[a]
Hsn	15.3 ± 21.8	1.4 ± 2.9	0.0008[a]
FDG-PET			
Maximal SUVmax at bone lesion	6.81 ± 3.42	2.47 ± 0.55	< 0.0001[a]
MTV			
in bone metastases	125.85 ± 257.70	0	
in visceral metastases	41.49 ± 78.69	39.56 ± 66.36	0.9464[a]
in the whole metastases	150.75 ± 296.27	8.21 ± 33.33	0.0005[a]
TLG			
in bone metastases	536.09 ± 1187.25	0	
in visceral metastases	196.86 ± 412.27	209.83 ± 398.97	0.9350[a]
in the whole metastases	652.30 ± 1414.65	43.46 ± 195.11	0.0017[a]

eGFR estimated glomerular filtration rate, *ALP* alkaline phosphatase, *CEA* carcinoembryonic antigen, *CA15*-3 carbohydrate antigen 15-3, *EOD* extent of disease, *ANN* artificial neural network, *BSI* bone scan index, *Hsn* number of positive hot spots, *SUVmax* maximum standardized uptake value, *MTV* metabolic tumor volume, *TLGa* total lesion glycolysis

[a]Student's *t* test

[b]Fisher's exact test

[c]Pearson's Chi-square test

Table 2 Patients' characteristics

	With visceral metastasis ($n=29$)	Without visceral metastasis ($n=59$)	p value
Bone scintigraphy			
EOD	1.45 ± 1.18	0.47 ± 0.75	< 0.0001[a]
ANN value	0.57 ± 0.43	0.30 ± 0.36	0.0024[a]
BSI	1.57 ± 2.40	0.38 ± 0.78	0.0008[a]
Hsn	12.72 ± 22.14	2.95 ± 6.58	0.0023[a]
FDG-PET			
Maximal SUVmax at bone lesion	4.35 ± 4.24	2.25 ± 2.72	0.0078[a]
MTV in bone lesions	92.78 ± 233.16	20.52 ± 108.80	0.0500[a]
TLG in bone lesions	399.48 ± 1086.08	85.32 ± 475.44	0.0310[a]

EOD extent of disease, *ANN* artificial neural network, *BSI* bone scan index, *Hsn* number of positive hot spots, *SUVmax* maximum standardized uptake value, *MTV* metabolic tumor volume, *TLG* total lesion glycolysis

[a]Student's *t* test

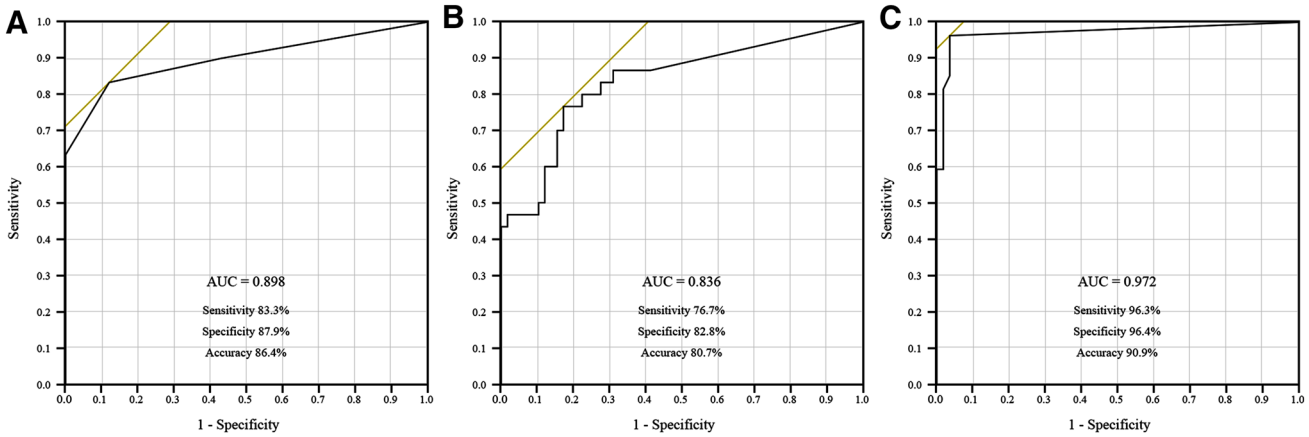

Fig. 2 The diagnostic accuracy of a bone scan with EOD and BSI and SUVmax on FDG-PET assessed by receiver operating characteristics (ROC) analysis with area under the curve (AUC). **a** EOD, **b** BSI, **c** SUVmax

and BSI (HR = 1.25), TLG in bone metastasis (HR = 1.0003) and TLG in the whole metastasis (HR = 1.0003) showed significantly higher risk ratios compared to the lower patients. Multivariate Cox proportional hazards ratio of the covariates are shown in Table 4. In the patients without visceral metastasis, high BSI (HR = 19.146) and high SUVmax (HR = 10.119) were independent prognostic factors. In the patients with visceral metastasis, high BSI (HR = 7.876, 95% CI 1.705–36.204) was the only independent prognostic factor.

Discussion

We clarified the diagnostic value of the ANN for detecting bone metastasis in patients with breast cancer. The ANN, a fully automated computer-aided diagnostic (CAD) system, could quantify potentially metastatic lesions from bone scans with high reproducibility, which suggested that not only the presence but also the extent of bone metastasis influence a patient's prognosis.

In the present study, we analyzed the relationship between the prognosis of the patients with breast cancer and the results of the bone scan that was quantitatively evaluated by the ANN. Since Soloway et al. indicated the correlation between the prognosis of the patients with prostate cancer and bone scan findings by using the extent of disease (EOD) [10], a large number of researchers have supported the usefulness of bone scan for cancer staging. Moreover, some studies suggested that the ANN, or CAD system, could identify probable metastatic lesions and therefore help to improve diagnostic accuracy, even if this was not a quantitative but qualitative evaluation [16, 17]. Most of the previous

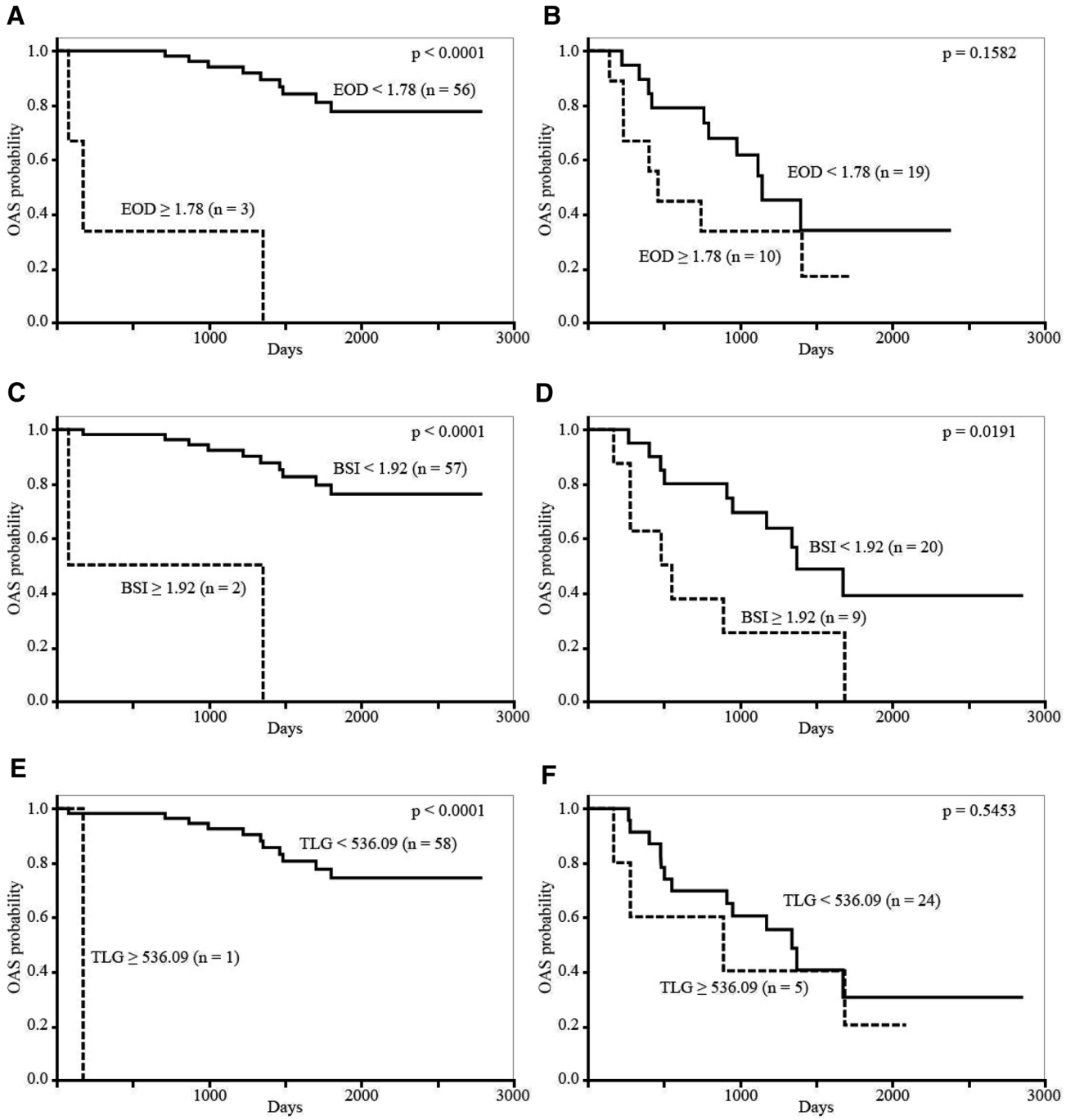

Fig. 3 Overall survival divided by EOD scale (< 1.78 vs. ≥ 1.78, **a** and **b**), BSI (< 1.92 vs. ≥ 1.92, **c** and **d**) and TLG (< 536.09 vs. ≥ 536.09, **e** and **f**) in the patient with and without visceral metastasis, respectively. Each cutoff value was determined by the mean value of patients with bone metastasis. **a**, **c** and **e** the patient without visceral metastasis. **b**, **d** and **f** patients with visceral metastasis

results, however, focused on prostate cancer metastases, which are disseminated in bones mainly with osteoplastic changes, whereas the detection of osteolytic or mixed osteolytic/blastic metastasis including metastatic breast cancer have shown poor results in terms of accuracy.

Bone scans with ANN technology may be helpful in improving not only overall survival but also progression-free survival of breast cancer patients with bone metastasis. Cohort studies and meta-analyses during the last decade demonstrated that breast and prostate cancer accounted for about 80% of all cases of bone metastasis [18]. In addition, bone metastasis from breast and prostate cancer might develop SREs more frequently than that of any other cancers. Statistically, more than a half of either breast and

Table 3 Univariate Cox proportional hazard analysis

	Range of values	Hazard ratio per unit	95% CI	*p* value
EOD	0–4	2.03	1.549–2.611	< 0.0001
SUVmax	1.0–13.0	1.20	1.099–1.307	0.0002
BSI	0.0–9.669	1.25	1.083–1.403	0.0045
TLG(bone)	0–5517.431	1.0003	1.00002–1.0005	0.0374
TLG(total)	0–6720.295	1.0003	1.000004–1.0004	0.0475
Serum ALP	97–1437	1.00	0.999–1.002	0.1769
CA15-3	5.5–441.3	1.00	0.998–1.005	0.1911
Serum calcium	7.9–10.7	0.59	0.291–1.367	0.2130
TLG(visceral)	0–1350.629	1.0008	0.9994–1.002	0.2190
CEA	0.0–108.1	1.01	0.991–1.023	0.2400

EOD extent of disease, *SUVmax* maximum standardized uptake value, *BSI* bone scan index, *TLG* total lesion glycolysis, *TLG*(*bone*) the summed value of TLG in bone metastases, *TLG*(*total*) the summed value of TLG in the whole metastases, *ALP* alkaline phosphatase, *CA15-3* carbohydrate antigen 15-3, *TLG*(*visceral*) the summed value of TLG in visceral metastases, *CEA* carcinoembryonic antigen

Table 4 Multivariate Cox proportional hazard analysis patients without visceral metastasis

	Hazard ratio	95% CI	*p* value
SUVmax (> 6.73)	10.12	2.097–37.889	0.0068
BSI (> 1.92)	19.15	2.567–97.736	0.0077
TLG(bone) (> 536.09)	17.00	0.574–519.448	0.0910
Patients with visceral metastasis			
	Hazard ratio	95% CI	*p* value
BSI (> 1.92)	7.88	1.705–36.204	0.0084
TLG(total) (> 251.02)	4.98	0.813–24.684	0.0791
TLG(bone) (> 536.09)	4.46	0.553–35.332	0.5490
SUVmax (> 6.73)	2.72	0.548–15.503	0.2189

SUVmax maximum standardized uptake value, *BSI* bone scan index, *TLG* total lesion glycolysis, *TLG*(*total*) the summed value of TLG in the whole metastases, *TLG*(*bone*) the summed value of TLG in bone metastases

prostate cancer patients with bone metastasis are considered to experience SREs within 5 years after the onset of bone metastasis [19, 20]. A bone scan with ANN technology may promote earlier intervention in breast cancer patients, hopefully leading to an extension in progression-free and overall survival.

ANN technology is considered to improve the diagnostic accuracy of metastatic bone tumors from breast cancer. The American Society of Clinical Oncology Clinical Practice Guidelines (ASCO Guideline) suggests that all imaging modalities except mammography are not recommended as routine breast cancer surveillance for early detection of metastasis, because the meta-analysis showed that they did not help in improving a patient's prognosis [21]. The limitation of diagnostic imaging modalities is considered to stem mainly from the difficulty in definite and reproducible evaluations from the initial assessment, therapeutic effects, and prognosis [22]. Considering such limitations ANN-based quantitative evaluation might resolve this problem and would contribute in increasing the diagnostic value of bone scintigraphy.

A bone scan evaluated by ANN technology might be superior to novel evaluation methods of FDG-PET in terms of reproducibility. Recently, FDG-PET for surveillance of metastatic breast cancer before and after surgery has gained in popularity. A number of studies have shown the effectiveness of FDG-PET for establishing an initial diagnosis [23], evaluating therapeutic effect to anticancer drugs [24, 25], re-staging [26], and predicting long-term prognosis [27]. Compared to bone scintigraphy, some studies have reported that FDG-PET/CT showed higher sensitivity and specificity for detecting bone metastasis [28]. Additionally, MTV and TLG have been used as novel scales instead of SUVmax in order to improve the accuracy of FDG-PET. While MTV and TLG can measure the extent and level of glucose metabolism in tumors quantitatively, these values might well vary according to the setting of the ROI and the threshold of SUVmax depending on inter-user reliability. Furthermore, it is sometimes difficult to confirm whether all the contoured regions by the threshold were metastatic lesions, especially in patients suspected of having multiple metastases. Although MTV and TLG were considered to be useful in this study as well as in many previous studies, bone scans evaluated by ANN are still considered to have higher reproducibility than these scales for evaluating the severity of bone metastasis.

Interestingly, regarding the presence of bone metastasis, despite much higher AUC values in TLG compared with those from the ANN or BSI, long-term observation showed that BSI might be a better prognostic factor than TLG. Because it is considered that BSI indicates the total amount of probable bone metastasis in the whole body even

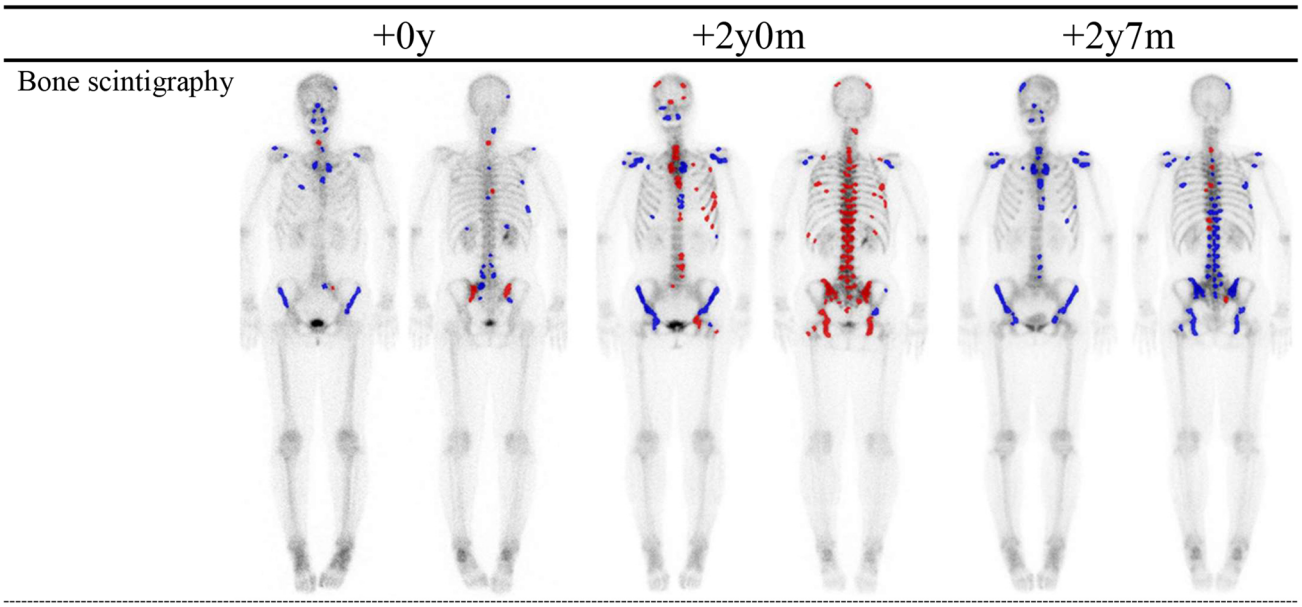

	+0y	+2y0m	+2y7m
ALP [IU/L]	390	691	202
Calcium [mg/dL]	9.7	9.9	9.5
CEA [ng/mL]	3.8	34.3	24.7
CA15-3 [U/mL]	18.7	225.1	144.3
ANN value	0.58	0.99	0.44
BSI	0.552	5.629	0.216
Hsn	4	64	7
SUVmax	4.00	3.05	3.39
TLG(bone)	6.4	3.7	46.6

Fig. 4 A 60-year-old female patient with breast cancer. No apparent metastasis had been found at the first examination after surgical operation (left column). However, 2 years after initial diagnosis (middle column), multiple bone metastases on CT and bone scan (upper row) and decreased uptake in osteoblastic lesions on FDG-PET (middle row) were detected. After changing anticancer agents (right column), BSI and tumor markers improved dramatically compared with SUVmax (lower row)

including those undetectable lesions in previous examinations, the long-term prognosis might be affected not only by the presence but more directly by the extent of bone metastasis. Figure 4 shows a patient's change evaluated by blood examination, bone scan, and FDG-PET. Considering tumor markers, a bone scan appears to be more suitable for assessing a patient's condition than FDG-PET. Potential roles of BSI for prognosis and FDG-PET for diagnosis could be demonstrated in this study. Further studies about

the sequential change of these unknown or uncertain lesions will therefore be required.

Some limitations should be mentioned for the use of ANN in this study. First, because we retrospectively evaluated the clinical use of the bone scan, the interval time from ^{99m}Tc-MDP injection to image acquisition varied by each patient. Shintawati et al. previously reported that the BSI and the number of the positive hot spots were highly affected by acquisition time [29]. Second, because ^{99m}Tc-MDP is excreted through the kidney, renal function might also influence the ANN. This may induce some discrepancy between the clinical course and BSI changes especially in follow-up studies. Third, a bone fracture has sometimes been diagnosed as a suspected metastasis. Since automated analysis was used to obtain reproducible results in this study, we did not exclude false-positive lesions, which could be excluded manually in accordance with CT findings. Because a bone scan and other modalities such as tumor markers and FDG-PET have a certain amount of non-specificity, exclusion of the non-specific accumulation of a bone scan based on other modalities was not always appropriate for evaluating the diagnostic value of a bone scan. Fourth, considering that SREs frequently shorten a patient's lifetime, it may be natural that the false-positive lesions of the ANN by bone fracture in the vertebrae influence the prediction of a patient's prognosis. Finally, we did not evaluate the relationship between a bone scan and treatment, which is clinically one of the most important issues to be investigated. Whether a decrease in BSI by anticancer therapy reflects an improvement in a patient's prognosis is still a consideration to the oncologist and should therefore be studied in future work.

Conclusion

BSI is calculated by a fully automated and CAD system and significantly correlates with the existence of bone metastasis. In patients with breast cancer, the patients with a high BSI had poor overall survival compared with those with a low BSI. Furthermore, BSI was an independent prognostic factor in patients with visceral metastasis from breast cancer.

Acknowledgements The authors thank Dr. Masafumi Inokuchi for his precise description of patients' clinical history

Funding None

Compliance with ethical standard

Disclosure K. Nakajima has a collaborative research work with FUJIFILM Toyama Chemical for developing BONENAVI software. Other authors have declared no conflicts of interest.

References

1. Rubens RD. Bone metastases–the clinical problem. Eur J Cancer. 1998;34(2):210–3.
2. Zeintl J, et al. Quantitative accuracy of clinical 99mTc SPECT/CT using ordered-subset expectation maximization with 3-dimensional resolution recovery, attenuation, and scatter correction. J Nucl Med. 2010;51(6):921–8.
3. Fukuoka M, et al. Comparison of diagnostic value of I-123 MIBG and high-dose I-131 MIBG scintigraphy including incremental value of SPECT/CT over planar image in patients with malignant pheochromocytoma/paraganglioma and neuroblastoma. Clin Nucl Med. 2011;36(1):1–7.
4. Erdi YE, et al. Quantitative bone metastases analysis based on image segmentation. J Nucl Med. 1997;38(9):1401–6.
5. Imbriaco M, et al. A new parameter for measuring metastatic bone involvement by prostate cancer: the Bone Scan Index. Clin Cancer Res. 1998;4(7):1765–72.
6. Zafeirakis AG, Papatheodorou GA, Limouris GS. Clinical and imaging correlations of bone turnover markers in prostate cancer patients with bone only metastases. Nucl Med Commun. 2010;31(3):249–53.
7. Wakabayashi H, et al. Bone scintigraphy as a new imaging biomarker: the relationship between bone scan index and bone metabolic markers in prostate cancer patients with bone metastases. Ann Nucl Med. 2013;27(9):802–7.
8. Nakajima K, et al. Enhanced diagnostic accuracy for quantitative bone scan using an artificial neural network system: a Japanese multi-center database project. EJNMMI Res. 2013;3(1):83.
9. Iwase T, et al. The relationship between skeletal-related events and bone scan index for the treatment of bone metastasis with breast cancer patients. Medicine (Baltimore). 2014;93(28):e269.
10. Soloway MS, et al. Stratification of patients with metastatic prostate cancer based on extent of disease on initial bone scan. Cancer. 1988;61(1):195–202.
11. Ethical Guidelines for Medical and Health Research Involving Human Subjects. Public notice of the Ministry of Education, Culture, Sports, Science and Technology and the Ministry of Health, Labour and Welfare No. 3 of 2014.
12. Ulmert D, et al. A novel automated platform for quantifying the extent of skeletal tumour involvement in prostate cancer patients using the Bone Scan Index. Eur Urol. 2012;62(1):78–84.
13. Sjostrand K, Ohlsson M, Edenbrandt L. Statistical regularization of deformation fields for atlas-based segmentation of bone scintigraphy images. Med Image Comput Comput Assist Interv. 2009;12(Pt 1):664–71.
14. Boellaard R, et al. FDG PET/CT: EANM procedure guidelines for tumour imaging version 2.0. Eur J Nucl Med Mol Imaging. 2015;42(2):328–54.
15. DeLong ER, DeLong DM, Clarke-Pearson DL. Comparing the areas under two or more correlated receiver operating characteristic curves: a nonparametric approach. Biometrics. 1988;44(3):837–45.
16. Sadik M, et al. Improved classifications of planar whole-body bone scans using a computer-assisted diagnosis system: a

multicenter, multiple-reader, multiple-case study. J Nucl Med. 2009;50(3):368–75.
17. Tokuda O, et al. Investigation of computer-aided diagnosis system for bone scans: a retrospective analysis in 406 patients. Ann Nucl Med. 2014;28(4):329–39.
18. Coleman RE. Bisphosphonates: clinical experience. Oncologist. 2004;9(Suppl 4):14–27.
19. Norgaard M, et al. Skeletal related events, bone metastasis and survival of prostate cancer: a population based cohort study in Denmark (1999–2007). J Urol. 2010;184(1):162–7.
20. Jensen AO, et al. Incidence of bone metastases and skeletal-related events in breast cancer patients: a population-based cohort study in Denmark. BMC Cancer. 2011;11:29.
21. Khatcheressian JL, et al. Breast cancer follow-up and management after primary treatment: American Society of clinical oncology clinical practice guideline update. J Clin Oncol. 2013;31(7):961–5.
22. Sadik M, et al. Quality of planar whole-body bone scan interpretations–a nationwide survey. Eur J Nucl Med Mol Imaging. 2008;35(8):1464–72.
23. Krammer J, et al. (18)F-FDG PET/CT for initial staging in breast cancer patients–Is there a relevant impact on treatment planning compared to conventional staging modalities? Eur Radiol. 2015;25(8):2460–9.
24. Groheux D, et al. F-FDG PET/CT in the early prediction of pathological response in aggressive subtypes of breast cancer: review of the literature and recommendations for use in clinical trials. Eur J Nucl Med Mol Imaging. 2016;43(5):983–93.
25. Ishiba T, et al. Efficiency of fluorodeoxyglucose positron emission tomography/computed tomography to predict prognosis in breast cancer patients received neoadjuvant chemotherapy. Springerplus. 2015;4:817.
26. Murakami R, et al. FDG-PET/CT in the diagnosis of recurrent breast cancer. Acta Radiol. 2012;53(1):12–6.
27. Son SH, et al. Whole-body metabolic tumor volume, as determined by (18)F-FDG PET/CT, as a prognostic factor of outcome for patients with breast cancer who have distant metastasis. AJR Am J Roentgenol. 2015;205(4):878–85.
28. Rong J, et al. Comparison of 18 FDG PET-CT and bone scintigraphy for detection of bone metastases in breast cancer patients. A meta-analysis. Surg Oncol. 2013;22(2):86–91.
29. Shintawati R, et al. Evaluation of bone scan index change over time on automated calculation in bone scintigraphy. Ann Nucl Med. 2015;29(10):911–20.

Affiliations

Anri Inaki[1] · Kenichi Nakajima[2] · Hiroshi Wakabayashi[1] · Takafumi Mochizuki[3] · Seigo Kinuya[4]

Kenichi Nakajima
nakajima@med.kanazawa-u.ac.jp

Hiroshi Wakabayashi
wakabayashi@staff.kanazawa-u.ac.jp

Takafumi Mochizuki
t.mochizuki@kadmedic.jp

Seigo Kinuya
kinuya@med.kanazawa-u.ac.jp

[1] Department of Nuclear Medicine, Kanazawa University Hospital, 13-1 Takara-machi, Kanazawa 920-8641, Japan

[2] Department of Functional Imaging and Artificial Intelligence, Kanazawa University, 13-1 Takara-machi, Kanazawa 920-8641, Japan

[3] Kanazawa Advanced Medical Center, 13-1 Takara-machi, Kanazawa 920-8641, Japan

[4] Department of Nuclear Medicine, Faculty of Medicine, Institute of Medical, Pharmaceutical and Health Sciences, Kanazawa University, 13-1 Takara-machi, Kanazawa 920-8641, Japan